Study on Seismic Wave Characteristics and Seismic Intensity Distribution of the 1923 Great Kanto Earthquake Using Multiple Source Model

— For the Improvement of Accuracy Concerned with the Estimation of Earthquake Disaster Prediction —

by

Takahisa Enomoto* and Toshio Mochizuki**

Table of Contents

ABSTRACT

It is very important to investigate the reasonable in-put seismic wave characteristics for the earthquake resistant design of structures in civil and building engineering and also for the earthquake disaster mitigation program. Recently, it will be a common understanding that the index keywords for specifying the in-put seismic wave characteristics reasonably are the properties of seismic source mechanism, path of wave propagation and ground condition directly under the site and its vicinities. So we think that it will be necessary to consider the convolution of above mentioned properties and we have to recognize the regional property individually. Then we are making the simple data base for underground condition using the topographical and geological data and some other references concerned with underground structure in the Kanto District where is the capital region in Japan.
In this paper, for the first step, we use the simulation method for evaluating the seismic wave characteristics and seismic intensity distribution of two middle-scale earthquakes occurred in this area and also the 1923 Great Kanto Earthquake theoretically using above mentioned data base and multiple source model.

Keywords: Great Kanto Earthquake, Seismic Wave Characteristics,
Seismic Intensity Distribution, Multiple Source Model

1. Introduction

One of the most basic and important items in designing the earthquake resistance of a structure is to determine the input seismic wave for the design in a reasonable manner, for the reason that this sometimes very much affects the structural design. In order to evaluate the input seismic wave at arbitrary points in the conventional method, source parameters are to be established compared with a number of observed records of middle- and small-scale earthquakes by using macroscopic fault model, and seismic zone needs to be studied while studying similarities of seismic wave characteristics. However, this model can hardly explain the characteristics of source in the case of a large-scale earthquake where the rupture process seems to be complicated, therefore a complicated behavior of the fault plane needs to be incorporated into the model. In such an earthquake, the specific barrier model[1)] (hereafter called the barrier model), which is one of the multiple source models that can explain the complexity of the fault movement by the uniformity, is often used in practice. Namely, a large-scale earthquake, such as the Great Kanto Earthquake (magnitude (M) = 7.9 by

*Faculty of Engineering, Kanagawa University
**Center of Urban Studies, Tokyo Metropolitan University

the Meteorological Agency) which is supposed to have had an extensive range of fault plane resulting from consecutive occurrence of a lot of earthquakes, can be expected to be explained by using this model. The fault plane of the Great Kanto Earthquake was estimated by H. Kanamori[2] from the aftershock distribution, and the complicated rupture on the fault plane can be explained in relation to the scale of the main shock and aftershock and also to the regional constancy of the middle- and small-scale earthquake obtained from the existing study. By taking these effects as parameters and comparing with the restored seismic wave record of the Great Kanto Earthquake, the seismic wave characteristics will be obtained in the same manner as those of the middle- and small-scale earthquake. Besides, using these source parameters and the underground model of the underground structure, such as that found in the earthquake damage assessment of Kanagawa Prefecture, makes it possible to estimate to some extent the maximum acceleration value and input seismic wave at an arbitrary point. This study, while paying attention to the Great Kanto Earthquake from the viewpoint of the above, aims at obtaining an estimate of the input seismic wave characteristics of the main shock and the seismic intensity distribution of the metropolitan area.

2. Progress and method of study

Hitherto in the past method, the regional constancy of seismic wave characteristics was obtained by examination of a number of records of middle- and small-scale earthquakes (M = 3 - 6) with hypocenter

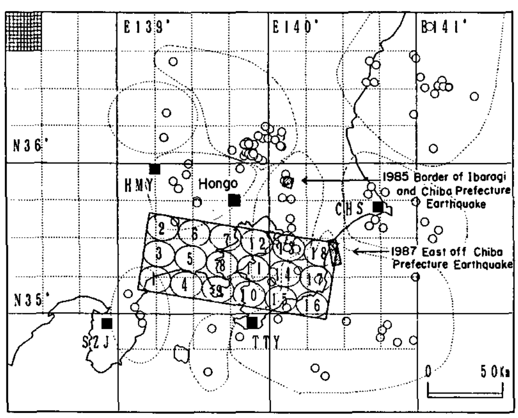

Fig.1 Location of fault plane and assumption of rupture[process concerned with the 1923 Great Kanto Earthquake

located in Kanto area as illustrated with small circle (O) in Fig. 1.[5] Thereafter, primary parameters are to be established and the seismic intensity distribution evaluated through the examination of the Kanto Earthquake using the multiple source model made with respect to the regionality.[6] However, since all of these studies are based on the analysis by the elastic calculation as regards the earthquake response calculation of the ground, this bring about various problems concerning precision of the parameters and evaluation of seismic intensity distribution. In this study, in respect to the above points, two middle-scale earthquakes, the 1985 earthquake on the Border of Ibaraki and Chiba Prefectures and the 1987 earthquake East Off Chiba Prefecture (M = 6.7), are analyzed using the multiple sources model as an attempt to verify the validity of the analytical method before dealing with a large-scale earthquake. Thereafter, they are subjected to the comparative study with restored records in the Hongo Campus of Tokyo University, and the source process of the Kanto Earthquake is evaluated with respect to the effect of surface wave. In addition, the underground structure of the metropolitan area is divided into surface ground and basement to make a modeling, and evaluation of the seismic intensity distribution of the Kanto Earthquake is carried out to compare with the actual damage distribution by taking into consideration the plastic effect through the dependence on strain of the surface ground. The average image obtained from numerous strong motion records is compared with the analytical results to verify the source parameters and precision of the analytical method.

3. Determination of ground structure

It is necessary to determine the magnitude of the earthquake, hypocentral distance, characteristics of source, propagation path, and also local underground structure in order to obtain the seismic intensity of an arbitrary point. In this study, the layered soil structure of the Kanto area is roughly divided into surface ground and basement for making a model, and parameters for each ground structure are determined mesh by mesh. The grid is drawn up by dividing the mesh of 1° latitude and longitude into 4 divisions, and further into 10 subdivisions of about 2.5 km x 2.5 km. The areas taken into the model are Tokyo and 6 prefectures, Kanagawa, Saitama, Chiba, Ibaraki, Tochigi, and Gunma, and the number of meshes amounts to 4,340 in total up to 36°40' north latitude. The classification of surface ground of Kanagawa Prefecture[4)] is roughly sorted into 5 kinds, sandy soil, clayey soil, Kanto loam, peat, and basement. These 5 soils have given representative transfer functions, therefore, appropriate parameters of the surface ground must be determined to match the above functions with the analytical ones. (Table 1) Taking into account the process and method of the classification of the representative transfer function, comparison with other prefectures as regards the transfer function of the surface ground is made to determine which category of the 5 kinds they fall in. For the prefectures whose transfer function was not available at that time, the map of soil classification was studied to find out which category each soil type on the map belongs to, and the surface ground of the metropolitan area is illustrated in these 5 kinds as shown in Fig. 2. The thickness of layer located under the surface was calculated from the contour map of Quarternary bottom face and the contour map of seismic basement obtained from the existing study based on the gelogical structure map in the latter Cenozoic era, and the existing values were used as for S wave velocity, density, and damping factor.

Table 1 Assumed parameters of classified of surface condition type

Classified Surface Ground Condition Type	Thickness (m)	S-wave Velocity (m/s)	Density (g/cm^3)	Damping Factor (Q)
Sandy Soil	25.00	250.00	2.00	10.00
Clayey Soil	18.00	200.00	1.90	10.00
Loam	25.00	200.00	2.10	10.00
Humus	15.00	150.00	1.90	10.00
Basement	18.00	400.00	2.20	20.00

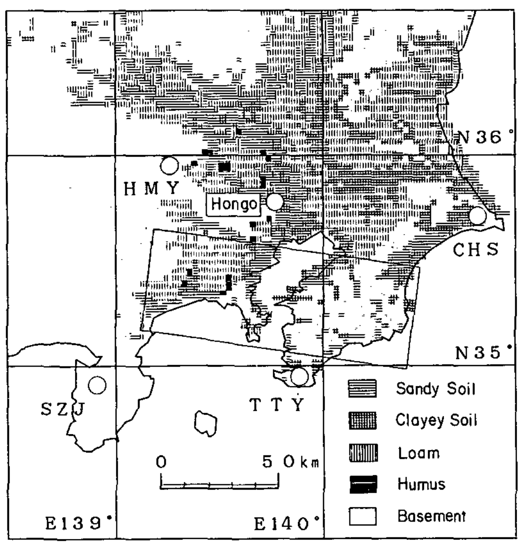

Fig.2 Map concerned with the distribution of classified surface ground condition

4. Study of middle-scale earthquakes

In this study, two earthquakes, the Earthquake East Off Chiba Prefecture and the Earthquake on the Border of Ibaraki and Chiba Prefectures, whose fault positions are marked with cross lines in Fig. 1, are studied while determining source parameters to establish, among other things, the study method of the Kanto Earthquake. In modeling the fault model, the multiple-source effect, which shows circular cracks being consecutively ruptured, was taken into consideration. The barrier model shown in Fig. 3 is used. The said

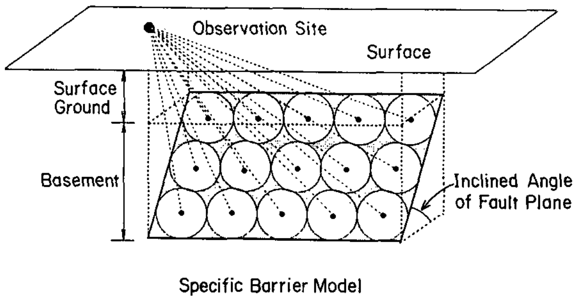

Fig.3 Conception of the multiple source model called Specific Barrier Model

model is assumed to have a rectangular fault plane made up of the assembly of small faults, i.e., circular cracks, and the clearance between small faults is regarded as a barrier. As rupture proceeds on the fault plane, rupture of crack is assumed to propagate. Addition of spectrum data produced from the individual circular cracks allows us to evaluate the seismic motion, therefore this model has often been used for a large-scale earthquake. Source parameters were repeatedly changed to closely approximate to the Fourier spectrum of the array observation measured at each observatory as shown in Fig. 1, Higashimatsuyama (HMY), Choshi (CHS),

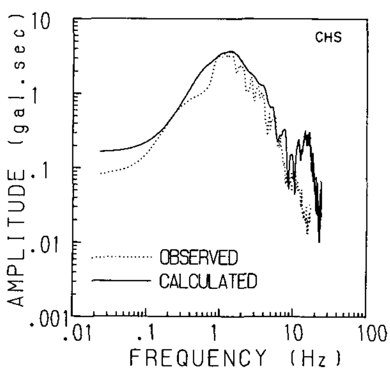

Fig.4 Comparison of Fourier concerned with the 1985 Border of Ibaragi and Chiba Prefecture Earthquake (M=6.1)

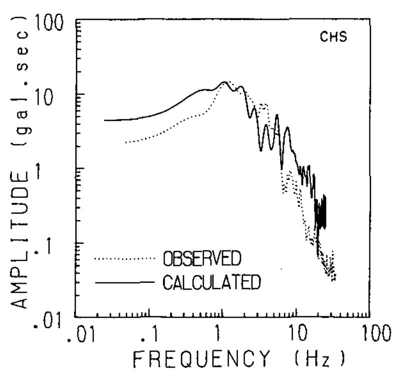

Fig.5 Comparison of Fourier Spectra concerned with the 1987 East off Chiba Prefecture Earthquake (M=6.7)

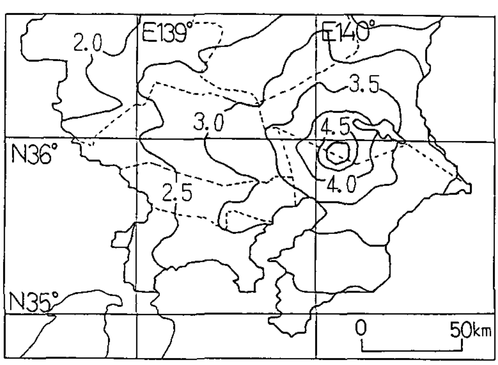

(a) The 1985 Border of Ibaragi and Chiba Prefecture Earthquake

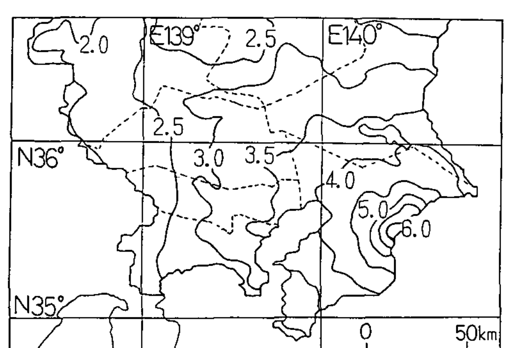

(b) The 1987 East off Chiba Prefecture Earthquake

Fig.6 Isoseismal maps indicated in JMA intensity scale by calculation method based on the multiple source model

Shuzenji (SZJ) and Tateyama (TTY), in due respect to the regional constancy obtained from the existing study, and only the body wave (S wave) was analyzed. It was found as a result that the analytical spectrum is coincident with that of the observed records at the observatory site (CHS) near the hypocenter of the earthquake as shown in Fig. 4 and Fig. 5. However, the iso-seismic map of the two earthquakes calculated from the maximum value of acceleration in each mesh appears to have larger distribution in particular at the point near the hypocenter than that (Fig. 7) of the existing study [9] [10] as shown in Fig. 6. Taking into account the above results, the Kanto Earthquake will be hereunder examined.

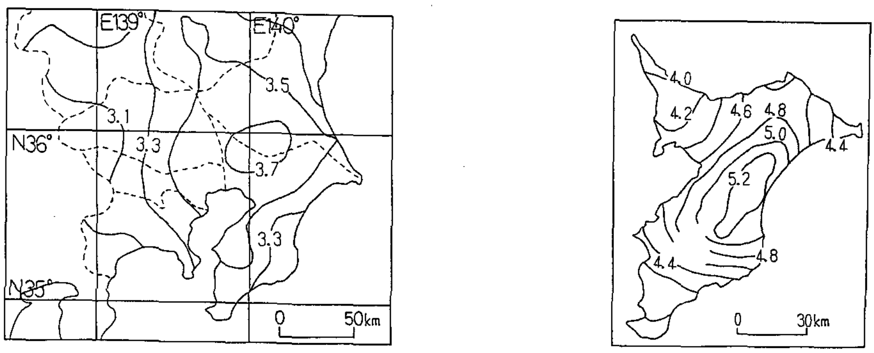

(a) The 1985 Border of Ibaragi and Chiba Prefecture Earthquake (b) The 1987 East off Chiba Prefecture Earthquake

Fig.7 Isoseismal maps indicated in JMA intensity scale by questionnaire survey of seismic intensity distribution based on the former investigations

5. Study of the Kanto Earthquake

5.1 Estimation method of fault model and parameters

As a fault plane model of the Kanto Earthquake, Kanamori's model [2] of which fault length is estimated at 130 km and fault width 70 km, as shown in Fig. 1, is adopted. M. Kamiyama has extracted average images of spectrum from among numerous strong motion records, examined the barrier model, and deducted the expected values of the acceleration Fourier spectrum. Based on the above, he has obtained the average radius and number of cracks on the barrier model.

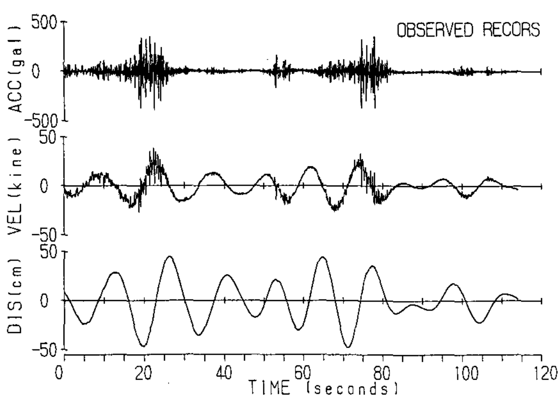

Fig.8 Synthetic seismic wave of the 1923 Great Kanto Earthquake by Morioka et al. based on the observed record at Hongo, University of Tokyo

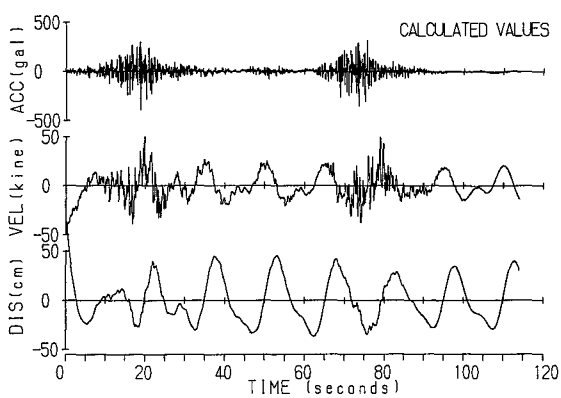

Fig.9 Synthetic seismic wave of the 1923 Great Kanto Earthquake based on the multiple source model

In this study, the number of circular cracks on the barrier model was set at 3 in south-north direction and 6 in east-west direction, amounting to 18 in total, according to the above study results, and the radius at about 11 km. Besides, the sequence of rupture was determined by trial and error on the assumption that rupture starts from near the west part of Kanagawa prefecture and Sagami Bay (N35.4° E139.2°), which is said to be the hypocenter of the Kanto Earthquake, and proceeds to the south-east direction in turn according to the number in Fig. 1. Source parameters are to be in general determined with due regard to the regional constancy estimated from the experimental formula and existing study results, and in this study they were determined through repeated operation until the analytical results become coincident with those of time history (Fig. 8) and Fourier spectrum of the observed record by T. Morioka and M. Yamada in the Hongo Campus of Tokyo University. As a result, each parameter used is tabulated in Table 2 and the theoretical seismic wave is shown in Fig. 9. Fig. 10 shows the contour line graduated by 3.2 bar line of local stress drop after being subjected to

Table 2. Assumed source parameters of the 1923 Great Kanto Earthquake

Order of Rupture Process	East Longitude (° ′ ″)	North Latitude (° ′ ″)	S-wave Velocity β (km/s)	Rupture Velocity Vr (km/s)	Radius of Circular Crack R_0 (km)	Rigidity μ (dyn·cm)	Stress Drop Δσ (bar)	Hypocentral Distance R (km)	Angle θ (°)
1	139,11,00	35,18,00	3.00	2.70	10.83	2.25E+11	12.00	67.1	57.6
2	139,19,00	35,38,00	5.00	6.50	10.83	6.25E+11	10.00	47.5	41.2
3	139,15,00	35,28,00	4.00	4.80	10.83	4.00E+11	25.00	53.2	47.6
4	139,24,00	35,14,00	3.00	3.60	10.83	2.25E+11	29.00	60.6	53.6
5	139,27,00	35,24,00	4.00	4.80	10.83	4.00E+11	12.00	45.3	36.9
6	139,30,00	35,34,00	5.00	2.50	10.83	6.25E+11	15.00	38.7	19.7
7	139,43,00	35,30,00	5.00	2.50	10.83	6.25E+11	15.00	37.5	13.4
8	139,39,00	35,20,00	4.00	4.80	10.83	4.00E+11	10.00	45.5	36.5
9	139,36,00	35,10,00	3.00	2.70	10.83	2.25E+11	10.00	61.6	53.8
10	139,49,00	35,06,00	3.00	2.70	10.83	2.25E+11	10.00	68.8	58.0
11	139,52,00	35,15,00	4.00	2.00	10.83	4.00E+11	15.00	55.7	47.6
12	139,56,00	35,25,00	5.00	2.50	10.83	6.25E+11	10.00	48.4	39.3
13	140,07,00	35,21,00	5.00	2.50	10.83	6.25E+11	15.00	62.2	52.2
14	140,05,00	35,11,00	4.00	2.00	10.83	4.00E+11	15.00	70.0	57.4
15	140,01,00	35,02,00	3.00	3.60	10.83	2.25E+11	10.00	80.6	62.9
16	140,14,00	34,57,00	3.00	3.60	10.83	2.25E+11	30.00	97.5	67.2
17	140,17,00	35,07,00	3.00	3.60	10.83	2.25E+11	30.00	86.2	63.8
18	140,20,00	35,17,00	3.00	3.60	10.83	2.25E+11	50.00	80.1	61.5

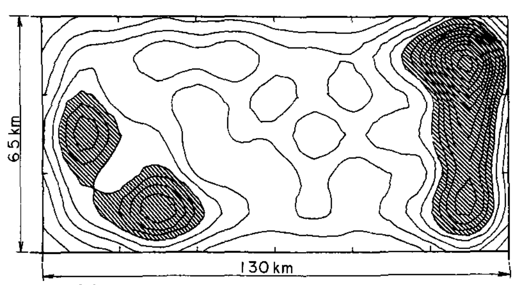

CONTOR LINES OF LOCAL STRESS DROP

Fig.10 Assumed distribution of the local stress drop on fault plane

averaging to some extent. The distribution of local stress drop on the fault plane was determined so that the point near the start and end points of rupture on the fault plane of the Kanto Earthquake become greater as shown with shadow part which is over about 20 bar. As for the underground structure at the analytical point of Hongo, the model uses one made by S. Midorikawa and H. Kobayashi [12] based on the investigation of deep underground structure by explosion experiment.

5-2 Comparative study of characteristics of seismic motion

Since the frequency characteristics of the theoretical seismic wave for body wave obtained in the previous section does not always match with those of the observed record, the surface wave of the underground structure of Hongo was newly established and intergrated with the body wave. It is found from Fig. 11 that

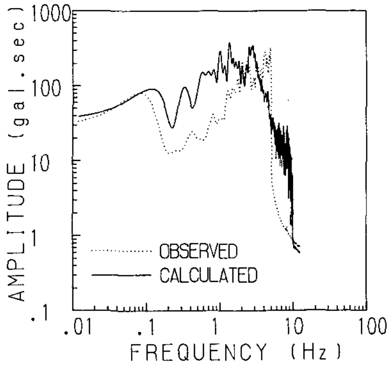

Fig.11 Comparison of the Fourier Spectra of seismic wave

frequency characteristics are almost coincident as a whole but show a difference of about 1 Hz on the high frequency range over 1 Hz. The running spectrum analysis shows the results of the comparision study between the calculation result and the observed record of acceleration in Fig. 12 and Fig. 13, in which the analytical result appears to be shifted by 1 Hz to the low frequency range side due to the above reason, but the strong motion phase is very much coincident. The reason why the above frequency characteristics were

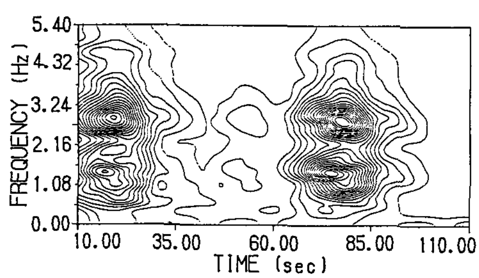

Fig.12 Result of the running Fourier spectral analysis concerned with the synthetic seismic wave based on multiple source model

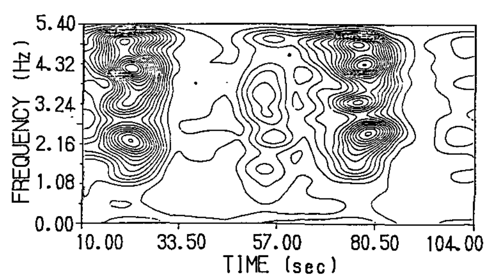

Fig.13 Result of the running Fourier spectral analysis concerned with the synthetic seismic wave based on observed record

obtained can be explained by several accounts, but it is partly attributable to the point that circular cracks with uniform size which simulate the complicate fault movement are uniformly arranged in the repture zone. Namely, this is because the barrier model is uniformly arranged, therefore, taking into consideration this point, the seismic wave by source parameter is regarded as coincident with that of the observed record.

5-3 Calculation of seismic intensity distribution

Since the seismic intensity distribution was calculated by the linear calculation in the aforementioned study of the middle-scale earthquake, comparatively greater values were taken as parameters at the point with smaller hypocenter distance. However, the plastic effect of soft surface ground can hardly be neglected at an acceleration level of the Kanto Earthquake with magnitude of as much as 8. Therefore, in this study, after elastic calculation in the conventional method, the analysis was made in the following method in order to evaluate the elastic effect of the only surface ground. As shown in Fig. 14, maximum acceleration value

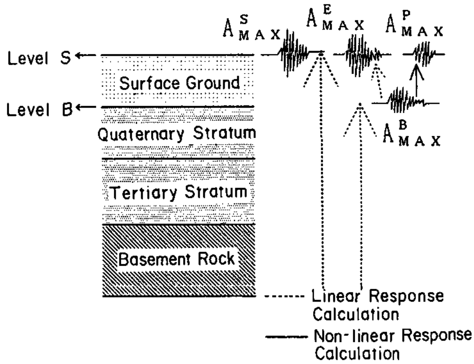

Fig.14 Conception for the treatment of effect concerned with the non-linear characteristics of soft surface sub-soil ground

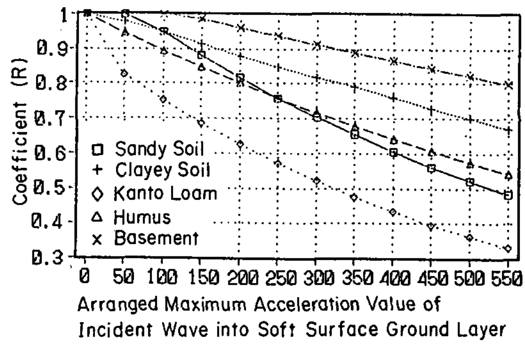

Fig.15 Distribution of coefficients (R) for the effect of non-linear characteristics concerned with classified surface ground condition types

A^B_{Max} is calculated at the analytical point of Hongo from the linear calculation on the underground model except for the surface ground. By taking the seismic wave for analysis at level B as input wave, elasto-plastic response calculation and elastic response calculation are carried out, under non-linear calculation program, for each parameter of 5 kinds of surface ground listed in Table 1. In order to assess the plastic effect corresponding to A^B_{Max} value, $A^B{}_{Max}$ is subjected to normalization by steps of 50 gal in a range of 50 gal to 550 gal, and A^P_{Max} and A^E_{Max} are calculated in elasto-plastic response calculation and elastic response calculation. Then, the ratio of the above two is calculated and coefficient R is obtained according to the breakdown by the maximum value and the soil type (5 kinds).

Table 3 Assumed coefficients (R) for the effect of non-linear characteristics concerned with classified surface-ground condition types

Arranged Maximum Acceleration Value (gal)	Classified Surface Ground Condition Type				
	Sandy Soil	Clayey Soil	Loam	Humus	Basement
0	1.00	1.00	1.00	1.00	1.00
50	1.00	0.98	0.82	0.95	1.00
100	0.95	0.95	0.75	0.89	1.00
150	0.88	0.91	0.69	0.85	0.99
200	0.82	0.88	0.63	0.80	0.96
250	0.76	0.85	0.57	0.76	0.94
300	0.70	0.82	0.52	0.72	0.91
350	0.65	0.79	0.48	0.68	0.89
400	0.61	0.76	0.43	0.64	0.87
450	0.56	0.73	0.40	0.61	0.84
500	0.52	0.70	0.36	0.57	0.82
550	0.48	0.67	0.33	0.54	0.80

Further, the above results are approximated for each soil type by regression curve using the least square method shown in Fig. 15. Coefficient R (Table 3) from regression curve which is determined by A^B_{Max} and the soil type of mesh is multiplied by the maximum value A^S_{Max} on the ground surface (S Level) obtained by the conventional linear calculation to compute the maximum acceleration value with respect to the plastic effect of the surface ground. The maximum acceleration value ($A_{Max} = A^{S}_{Max} \times R$) obtained by the above analytical method was subjected to conversion as for all meshes into seismic intensity by the expression for transfer

$$I_{JMA} = (\mathrm{Log}\,(A_{Max}) + 0.35) \times 2.0) \quad \ldots\ldots\ (1)$$

which converts into JMA Intensity Scale by H. Kawasumi in order to examine seismic intensity distribution . In addition, after smoothing the above results by the fitting method of quadratic curved surface, an iso-seismal map was drawn up as illustrated in Fig. 16. This iso-seismal map takes into account the plastic effect of the surface ground and is extremely coincident with the ratio of destroyed wooden houses in the Kanto Earthquake as shown in Fig. 17 as far as the area with high seismic intensity is concerned.

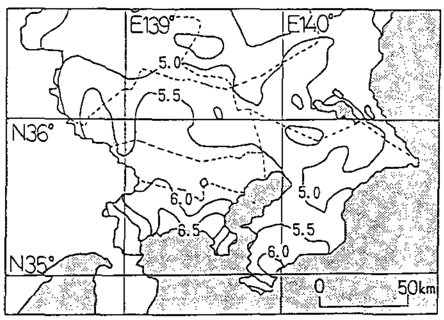

Fig.16 Isoseismal map of the 1923 Great Kanto Earthquake based on the synthetic seismic wave using the multiple source model

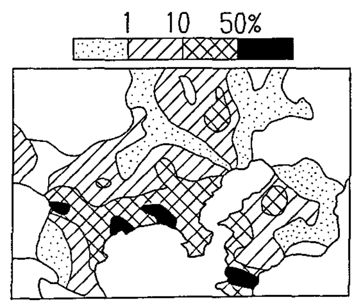

Fig.17 Contour map of the destroyed wooden houses in the 1923 Great Kanto Earthquake

5-4 Comparison of design averaged response spectra and attenuation

In contrast to seismic wave characteristics and seismic intensity distribution of the Kanto Earthquake calculated by the above method, design-use averaged response spectra and attenuation were compared. In the General Project "Development of the new earthquake resistant design", average image of input seismic wave in Japan is given. The averaged response accelerational spectrum with respect to the classification can be obtained by the magnitude and epicentral distance from seismic wave of 227 elements acquired on various soil types. Fig. 18 shows the comparison between the above average spectrum and the analytical results at Hongo point, and it is found that they coincide very well. On the other hand, Fig. 19 describes the comparison of the

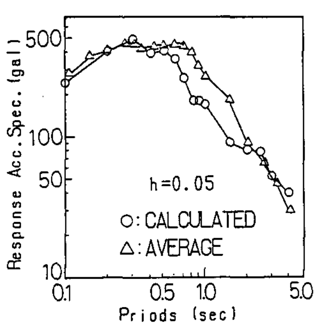

Fig.18 Comparison between the acceleration response spectra (h=5%) based on the proposed specific code for earthquake resistant design and synthetic seismic wave by multiple source model

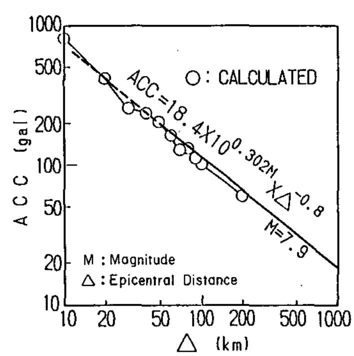

Fig.19 Comparison between the attenuation relations of maximum acceleration value based on the proposed specific code for earthquake resistant design and synthetic seismic wave by multiple source model

attenuation curve of the maximum acceleration value calculated from regression analysis of 301 pieces of strong motion record which have occurred in Japan with that calculated from this analysis. The maximum acceleration distribution in this study is limited to 200 km range and is not applicable to the range of the epicenter distance (Δ) of less than 50 km on the attenuation curve. However, both appear to coincide very well in a range of 50 km – 200 km. The above coincidence is likely to show that the parameter setting in this study was appropriate and the analysis was precise.

6. Conclusions

In this study, seismic wave characteristics as for a middle-scale earthquake and seismic intensity distribution were estimated using the multiple source model while varying source parameters with reference to the regionality of the seismic wave characteristics obtained from the study of middle- and small-scale earthquakes, which are based on array observed record. Then, taking into account these study results, the seismic wave characteristics of the Kanto Earthquake were reconsidered on the multiple source model and seismic intensity distribution was calculated with regard to the plastic effect of the surface ground. As a result, input wave characteristics were very well evaluated by this method. Therefore, this attests that the analytical methods in this study, including calculation method of seismic intensity distribution, were almost appropriate and carried out with precision, which provides the broad picture of seismic wave characteristics of the Great Kanto Earthquake, and it will be also helpful for the study of input seismic wave for design and earthquake disaster mitigation program.

<References>

1) Parageorgiou A.S., Aki K.; A specific barrier model for quantitative description of inhomogenious faulting and the prediction of strong ground motion I. Description of the model, Bulletin of the Seismological Society of America, Vol.73, No.3, 1983, PP.693-722

2) Kanamori H,, Ando M.; Fault parameters of the Great Kanto Earthquake of 1923, Publication for the 50th Anniversary of the Kanto Earthquake, 1923, The Earthquake Research Institute, University of Tokyo, PP.89-101

3) Morioka T., Yamada M.; Attempt to estimate the maximum ground motion of the Great Kanto Earthquake of 1923, Proc. of the 7th Japan Earthquake Engineering Symposium, 1986, PP.109-114

4) Kanagawa Prefecture; Report on the estimation of earthquake damages in Kanagawa Prefecture (Geological ground condition), 1985

5) Sasamoto O., Fujimoto M., Mochizuki T., Enomoto T.; On earthquake wave characteristics at the rock based on the earthquake records by array observation system Part 9. On the regional characteristics of source parameter Summaries of Technical Papers of Annual Meeting, Architectural Institute of Japan, 1990, PP.301-302

6) Sasamoto O., Mochizuki T., Enomoto T., Fujimoto M.; Study on the seismic intensity distribution of the 1923 Great Kanto Earthquake by using multiple source model, Summaries of Technical Papers of Annual Meeting, Architectural Institute of Japan, 1991, PP.515-516

7) Land Agency of Japan; The classification map of ground condition (1;200,000), Japan Map Center, 1991

8) Geological Survey of Japan; Tectonic Maps Series 2, Neotectonic Map Tokyo 1;500,000, 1973

9) Goto N., Kawachi K., Muto A., Komiyama H.; High density survey of seismic intensity distribution - The October 4th, 1985 southern part of Ibaraki Prefecture Earthquake -, Program and Abstract, The Seismological Society of Japan, 1987, No.1, P.278

10) Mochizuki T., Taniuchi Y., Shiono K., Ehara N.; On the seismic intensities and damages in Chiba Prefecture by the 1987 East off Chiba Prefecture Earthquake, Comprehensive Urban Studies, Tokyo Metropolitan University, No. 35, 1988, PP.5-31

11) Kamiyama M.; Earthquake source characteristics inferred from the statistically analyzed spectra of strong motions with aid to dynamic model of faulting, Proc. of the Japan Society of Civil Engineering, No.386/I-8, 1987, PP.175-184

12) Midorikawa S., Kobayashi H.; On estimation of strong earthquake motions with regard to fault rupture, Transactions of the Architectural Institute of Japan, No.282, 1979, PP.71-81 Earthquake engineering data, Proc. of the 6th Japan Earthquake Engineering Symposium, 1982, PP.265-272

14) Ministry of Construction; Proposal of the new earthquake resistant design method, Technical Research Report of General Project for the Development of New Earthquake Resistant Design, 1977

多重震源モデルによる1923年関東大地震の地震動特性の再検討と震度分布に関する研究

——地震災害予測評価の精度向上に向けて——

荏 本 孝 久*
望 月 利 男**

要　　約

地震災害予測評価の際には、想定地震を設定した上で地震動特性を評価する場合が多く、関東地方においては1923年関東大地震（M＝7.9）を対象とするケースが一般的である。このように地震災害予測評価を試みる場合に地震動特性の設定は基本的に重要である。これまで地震災害予測の観点から、任意の地点の地震動特性を設定する際に、特定の地震動の観測記録を利用したり、耐震設計用の平均化された地震動を採用する場合が多い。しかしながら、予測精度をより向上させるためには、想定される地震の特徴を反映した地震動特性の設定が望まれる。

本研究は、以上の観点から1923年関東大地震の地震動特性の再検討と震度分布についての検討を試みたものである。著者らは、これまでに巨視的断層モデルと地盤構造モデルを用いて関東地方およびその周辺に発生した多数の中小規模地震の地震動観測記録と比較しながら震源パラメータを推定し、地震動特性の類似性から震源区域を把握する試みを実施してきた。しかし、破壊過程が複雑であると考えられる関東大地震のような大規模な地震については、上記震源区域を包含するような断層面上において、複雑な破壊過程を震源パラメータの不均一性としてモデルに取り入れる必要があると考えられる。

本研究では、断層運動の複雑さを破壊強度の不均一性で説明する多重震源モデルとしてバリアーモデルを採用して検討を行うことにした。その際、関東大地震のような大規模な地震を扱う前に、本解析方法の有効性を確認するために、比較的最近発生した1985年茨城・千葉県境地震（M＝6.1）、1987年千葉県東方沖地震（M＝6.7）の２つの中規模な地震について、上記多重震源モデルにより震源パラメータを設定しながら、算定した地震動特性と震度分布について、強震観測記録に基づく地震動特性と既往の研究により推定された震度分布を比較検討した。さらにこれらの検討結果を考慮し、関東大地震について同様な多重震源モデルを用いて、復元された関東大地震の観測記録と比較しつつ本地震の地震動特性の再検討を行った。そして、良好な再検討結果が得られた多重震源モデルの震源パラメータを用いて関東地方の震度分布を算定した。その結果、本方法により関東大地震の地震動特性を良好に評価するとともに、震度分布についてもほぼ良好に説明できることを示すことができ、地震災害予測評価の精度向上に向けて、本方法による地震動特性と震度分布の評価方法が有効な方法となり得ることを示した。

＊神奈川大学工学部・東京都立大学都市研究センター非常勤研究員
＊＊東京都立大学都市研究センター